Online ISSN: 2588-3526

Journal of Wildlife and Biodiversity

Volume 7 (Special Issue): 138-155 (2023) (http://www.wildlife-biodiversity.com/)

Research Article

Synthesis, Characterization and Biological activity of mixed ligand Dimedon and Isatin with metal complex

Marwah M. Al-Dulaimi *, Omar H. Al-Obaidi

[1]Department of Chemistry, College of Science, Anbar University, Ramadi, Iraq

[*]Email: mhdymrwt65@gmail.com

Received: 27 August 2023 / Revised: 16 October 2023 / Accepted: 30 September 2023/ Published online: 25 November 2023.

How to cite: Al-Dulaimi, M.M., Al-Obaidi, O.H. (2023). Synthesis, Characterization and Biological activity of mixed ligand Dimedon and Isatin with metal complex, Journal of Wildlife and Biodiversity, 7 (Special Issue), 138-155. **DOI**: https://doi.org/10.5281/zenodo.10211625

Abstract

New compounds of mixed ligand complex (Scheme 1) were synthesized by the reaction of metal ions Zn (II), Cd (II), Co (II), Mn (II), Ni (II) Cu (II) and Fe (II) with the Dimedon (L1) as a primary ligand and Isatin (L2) as a secondary ligand in a molar ratio of 1:1:1 and identified using several spectral analysis methods, where used UV-visible, CHNOS elemental analysis, FT-IR, molar conductivity, mass spectrum, magnetic susceptibility and additionally, Chloride content as a quantitative evaluation, according to the results obtained by analysis methods, we observed that all the synthesized complexes showed apparent stability, an octahedral structure is suggested for all the prepared complexes, anti-bacterial and anti-fungal activities of these metal complexes were evaluated against Escherichia Coli, Spuedomonas (Gram-negative bacteria), Bacillus sp., Staphylococcus aureus (Gram-positive bacteria) and Fuzarium, Aspergillus a fungal species. The samples of the cultivated complexes showed varying results from the inhibition zone, and a similar one showed its ineffectiveness in inhibiting the growth of bacteria or fungi according to the concentrations prepared.

Keywords: Mixed ligand complex, Dimedon, Isatin, Anti-microbial

Introduction

Mixed ligand complexes play an important role in many chemical and biological systems such as water filtration, ion exchange resin, electroplating, antioxidants, photosynthesis in plants, and removal of unwanted and harmful metals from organisms (Taghreed et al.,2016) Many of these metal complexes show good biological activity against pathogenic microorganisms (Numan et

al., 2017). Mixed ligand complexes are suitable for simulating the role of metal ions, detoxification mechanisms, and drug design. New mixed ligand complexes are constantly being studied to obtain biologically active compounds (Numan,2015). Study of antipyrene and its derivatives. These compounds can act as antiparasitic agents and their complexes with platinum (II) and cobalt (II) ions have been shown to act as antitumor agents (Pandeya et al.,2005). This prompted them to synthesize ligands containing an anti-pyrinyl moiety in addition to the non-localized conjugate system followed by mixing it with 2-aminopyrene (2-AMPI), 8-hydroxyquinoline or oxalic acid with some of the investigated divalent and trivalent transition metal compounds(Ibrahim, 2015). For antifungal and antibacterial activities. Dimidone is an organic compound with the formula (CH3)2C(CH2)2(CO)2(CH2). It is classified as a cyclic diketone, which is a diketone derivative of 1, 3-cyclohexane. It is a white solid that is soluble in water, as well as ethanol and methanol. It was once used as a reagent to test for aldehyde functional groups, It is stable in ambient conditions and soluble in water, as well as in ethanol and methanol (JMOZINGO,1986). Dimidone and its derivatives have many biological properties such as anticarcinogenic, antioxidant, antihistamine and anticoagulant. During the oxidation process, chemiluminescence was observed, which belonged to 4-peroxydimidone radicals obtained from the first-step oxidation(Rao et al.,2021). Isatin or 1H-indole-2,3-dione, is an indole derivative that contains a keto group at positions 2 and 3 of the ring. The Isatin ring system consists of a pyrrole ring fused to a benzene ring. Isatin was first synthesized by Erdman and Laurent in 1841 by oxidation of indigo with nitric and chromic acids(Vandana et al.,2017). The compound is found in several plants, such as Isatis tinctoria and Calanthe and in Couroupita guianensis. Substituted isatins are also found in plants, eg methoxy phenylpentyl isatins (methoxy phenylpentyl isatins) in Melochia tomentosa. Isatin is also found in the human body because it is a metabolic derivative of adrenaline (Tadayon & Garkani-Nejad.,2019) The prepared complexes were characterized by different analysis methods , FT-IR, mass spectrum, UV-Vis spectrum, molar conductance, magnetic susceptibility and CHNOS elemental analysis. the metal ions (Zn (II), Cd (II), Co (II), Mn (II), Ni (II) Cu (II) and Fe (II)) reacted with the Dimedon (L1) as a primary ligand and Isatin (L2) as a secondary ligand in a molar ratio of 1:1:1, the formula of complexes [M (L1)(L2)(H2O)n] have been synthesized and the complexes showed octahedral geometries. The ligand and its complexes were screened against some bacterial species, Escherichia Coli , Spuedomonas (Gram-negative bacteria), Bacillus sp. ,

Staphylococcus aureus (Gram-positive bacteria) and Fuzarium, Aspergillus a fungal species, and the screened results showed different results in terms of the ability to inhibit pathogenic bacteria and fungi.

Martial and methods

All the starting materials, chemicals and solvents for the prepared compounds were of analytical grade. Absolut ethanol, methanol, DMSO and other solvents were of high purity and supplied by Merck Co. , Fluka Co. and Sigma-Aldrich Co. , Dimedon , Isatin and metal salts [FeCl3, ZnCl2, CoCl2.6H2O, MnCl2.4H2O, NiCl2.6H2O, CuCl2.2H2O and CdCl2.H2O] were supplied by Sigma-Aldrich Co. and BDH Co., The melting point of the prepared ligands and complexes were measured by a Stuart electrothermal melting point apparatus by capillary tube at Anbar University - College of Science - Department of Chemistry. The elemental (H, N, O, S, C) micro-analysis, to search using the EA 3000 single V.3 model vector device. Osingle Eure in the laboratories of Cairo University Microanalysis Center, Egypt. The chlorine content of the prepared complexes was measured using Mohr's method processor at Ibn Sina Laboratories, Baghdad. The mass spectra of the complexes were recorded using the LC-MSQP50A(E170ev) Shimadzu device in the laboratories of the University of Tehran, Iran. Infrared spectra were measured with a device (Shimadzu-8000S) and the ultraviolet-visible spectra of the ligand and its complexes were recorded using a Shimadzu UV-visible spectrophotometer, within a wavelength (200-1100) using a quartz cell with a path length of (1 cm) using a solvent such as DMSO dimethylformamide at a concentration of 1 × 10-3 M at Laboratories of the Ministry of Science, Department of Environment and Water Technology, Baghdad. The molar electrical conductivity of the prepared complexes dissolved in DMSO dimethylformamide was measured at a concentration of 1×10-3 molar and at the laboratory temperature using the BC3020 Professional Bench Top Conductivity device in the laboratories of the Department of Chemistry, College of Science for Women- University of Baghdad.

Synthesis of mixed ligand complex

In a round-bottomed flask with a capacity of (100 ml) put (0.237 g , 1 mmol) of CoCl2.6H2O dissolved in (10 ml) absolute ethanol with heating to complete the dissolution process, and at the same time with continuous stirring ligandin (0.140 g, 1 mmol) of Dimedon dissolved in (20 ml)

of ethanol and (0.177 g, 1 mmol) of Isatin dissolved in (20 ml) of ethanol, the mixture was left in the reflux process for an hour at a temperature (50Co) to form a brown precipitate, filtered the formed precipitate was dried and recrystallized using absolute ethanol at a ratio of (1:1:1) and weighed, so the resulting complex ratio was (60%)(Hegade et al.,2022). The rest of the complexes were prepared by dissolving the chlorides of the metal ions. Mn(II), Fe(III), Ni(II), Cu(II), Zn(II) and Cd(II) the same way.The steps of the preparation of the compounds are illustrated in Scheme (1).

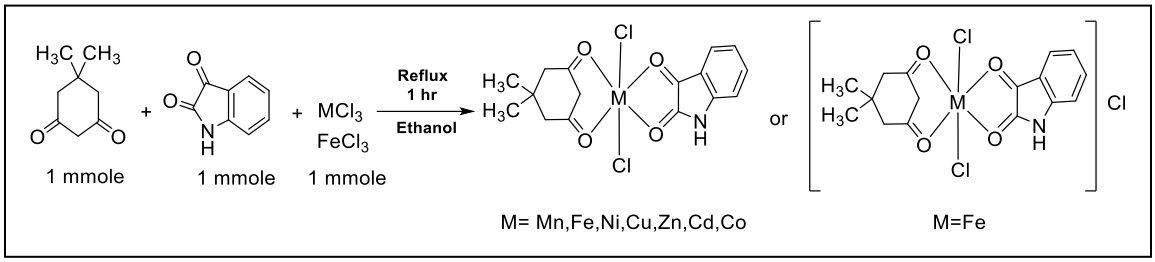

Scheme 1. The reaction sequences of prepared complexes

Antimicrobial activity test

In this study, the biological activities of the prepared complexes were tested in DMSO, as a solvent, and the complexes were evaluated using disc diffusion experiments against the growth of Escherichia Coli, Spuedomonas Gram-negative bacteria and Bacillus sp., Staphylococcus aureus Gram-positive bacteria, and the fungi Fuzarium, Aspergillus.

the bacterial and fungal isolates were collected from Anbar University, Department of Biology, College of Science, In Vitro assay was achieved by well diffusion method(Fatima et al.,2018; Matuschek et al.,2018). using different concentrations of the complexes of (0.0048, 0.0018, 0.0063, 0.0095, 0.0013, 0.0063 and 0.008) mg/mL in DMSO. The inhibition zones in mm illustrated in Table 5. The culture media was prepared for the growth of fungi according to instructions of the manufacturer, and then the inhibitory effectiveness of the complexes was tested by using different concentrations of the complexes (0.0048, 0.0018, 0.0063, 0.0095, 0.0013, 0.0063 and 0.008) mg/mL in DMSO as showed in Table 6

Results and discussion

The metal complexes were prepared by the reaction of Dimedon with Isatin and metal salts (FeCl3, ZnCl2, CoCl2.6H2O, MnCl2.4H2O, NiCl2.6H2O, CuCl2.2H2O and CdCl2.H2O) added in the ratio of 1:1:1. The complexes were characterized by using means of elemental analysis methods Elemental microanalysis C. H. N. O. S, infrared, UV-Vis spectra, Mass Spectrum, magnetic susceptibility and Molar Conductivity Measurements.

Elemental microanalysis, Chloride content and physical properties of the complexes

The data of element analysis (C .H .N .O .S) and Chloride content of the solid complexes prepared and The chlorine content of the synthesized complexes were measured using Mohr's method(Yilmaz & Topcu 1997) . the results were included of the analysis are in Table 1 Comparing the values obtained practically with those calculated theoretically clearly shows the great convergence, which makes the proportions of the elements in the complexes correct. The results of the silver nitrate (AgNO3) test for the chloride ion were negative, suggesting that the ion is not in the coordination sphere (Patange et al.,2008). As shown in Table 1. Also checked some physical features (color and melting points) for the complexes as shown in Table 2

Table 1. Element analysis (C. H. N. O. S) and Chloride content of synthesized complexes

Comp.	Calc.	C%	H%	N%	O%	S%	Cl%	M%
$[NiL_1L_2Cl_2]$= 416.91	Prac.	45.55	3.89	4.01	16.33	-	16.68	13.54
$C_{16}H_{17}NCl_2NiO_4$	Theor.	46.09	4.11	3.36	15.35	-	17.01	14.08
$[CoL_1L_2Cl_2]$= 417.15	Prac.	45.44	3.42	4.55	16.22	-	16.42	13.95
$C_{16}H_{17}NCl_2CoO_4$	Theor.	46.07	4.11	3.36	15.34	-	17.00	14.13
$[ZnL_1L_2\ Cl_2]$= 423.61	Prac.	46.05	3.49	4.44	16.08	-	15.77	14.17
$C_{16}H_{17}NCl_2ZnO_4$	Theor.	45.37	4.05	3.31	15.11	-	16.74	15.44
$[CuL_1L_2Cl_2]$ = 421.76	Prac.	45.54	3.55	4.44	14.89	-	16.66	14.92
$C_{16}H_{17}NCl_2CuO_4$	Theor.	45.56	4.06	3.32	15.17	-	16.81	15.07
413.15 $[MnL_1L_2Cl_2]$ =	Prac.	45.77	3.84	4.88	14.85	-	16.58	14.08
$C_{16}H_{17}NCl_2MnO_4$	Theor.	46.51	4.15	3.39	15.49	-	17.16	13.30

$[CdL_1L_2Cl_2]$= 470.96	Prac.	41.14	4.08	3.00	12.45	-	16.08	23.25
$C_{16}H_{17}NCl_2CdO_4$	Theor.	40.83	3.64	2.98	13.60	-	15.07	23.89
$[FeL_1L_2Cl_2]Cl$= 449.51	Prac.	41.77	4.55	4.44	13.38	-	22.88	12.98
$C_{16}H_{17}NCl_3FeO_4$	Theor.	42.75	3.81	3.12	14.24	-	23.66	12.42

Table 2. Some physical features (color and melting points) for the complexes

No.	Metal Salt	Weight of salt (mmole 1g)	Complex	Ylied%	Color	M.P.C Decomposition
1	$MnCl_2.H_2O$	0.197	$MnL_1L_2Cl_2.H_2O$	70	Yellow	212 – 214
2	$FeCl_3$	0.162	$FeL_1L_2Cl_3$	72	Dark brown	298 – 301
3	$CoCl_2.6H_2O$	0.237	$CoL_1L_2Cl_2.H_2O$	65	Purple	280 – 283
4	$NiCl_2.6H_2O$	0.237	$NiL_1L_2Cl_2.H_2O$	49	Yellow	410 – 412
5	$CuCl_2.2H_2O$	0.170	$[CuL_1L_2Cl]Cl$	63	Green	300 – 303
6	$ZnCl_2$	0.136	$[ZnL_1L_2Cl]Cl$	47	Pale Yellow	289 – 291
7	$CdCl_2.H_2O$	0.201	$[CdL_1L_2Cl]Cl$	60	Pale Yellow	288 – 290

FT-IR spectroscopy

FT-IR absorption spectra of the synthesized complexes were identified by infrared spectroscopy using dry potassium bromide (KBr) to determine the chemical elements in the prepared compounds. The metallic complexes were characterized spectrophotometrically by means of FT-IR infrared spectrum, where figures from (1) to (7) of the prepared complexes were shown to the appearance of the absorption spectrum of the adsorption-vibration-stretching bonding ν (M-O) within the range (445-582) cm-1 (Cozzi,2004). for the prepared complexes, and the appearance of an absorption band ν (C=O) within the range of cm-1 (1610-1683) (Teixeira et al.,2019). for the complexes, the appearance of an absorption band ν (N-H stretching vibration) within the frequency range of cm-1 (3390-3428)(Al-Hazmi et al.,2020). for complexes, also ν(C-H) Aliphatic absorption bands. Within the range of (2837-2995) cm-1, ν(C-H) Aromatic absorption bands also appear in the range of (2939-3176) cm-1 (Jirjees et al.,2021). The appearance of all these bands is preliminary evidence of the validity of the method of preparing these complexes, as shown in Table 3 values of the absorption spectrum bands

Table 3. the absorption spectrum bands data of m for synthesized complexes

No.	Comp.Symb.	ν(N-H)	ν(C-H) Arom.	ν(C=O)	ν (M-O)	ν(C-H) Alipha.
1	$[NiL_1L_2Cl_2]$	3427 wb	3082 3028 ws	1622 ws	572, 468 ws	2948 ws
2	$[CoL_1L_2Cl_2]$	3427 wb	3176 ws	1651 wsh	542, 460 497 ws	2995 ws
3	$[ZnL_1L_2Cl_2]$	3402 mb	3025 ws	1618 ws	542, 474 ws	2935 ws
4	$[CuL_1L_2Cl_2]$	3406 mb	3029 ws	1610 ws	582, 478 ws	2922 ws
5	$[MnL_1L_2Cl_2]$	3408 b	3016 mb	1610 msh	565 ws	2918 mb
6	$[CdL_1L_2Cl_2]$	3428 b	3029 wsh	1613 ws	567, 476 ws	2931 mb
7	$[FeL_1L_2Cl_2]Cl$	3390 b	2939 wsh	1683 msh	563,511,445 ws	2837 mb

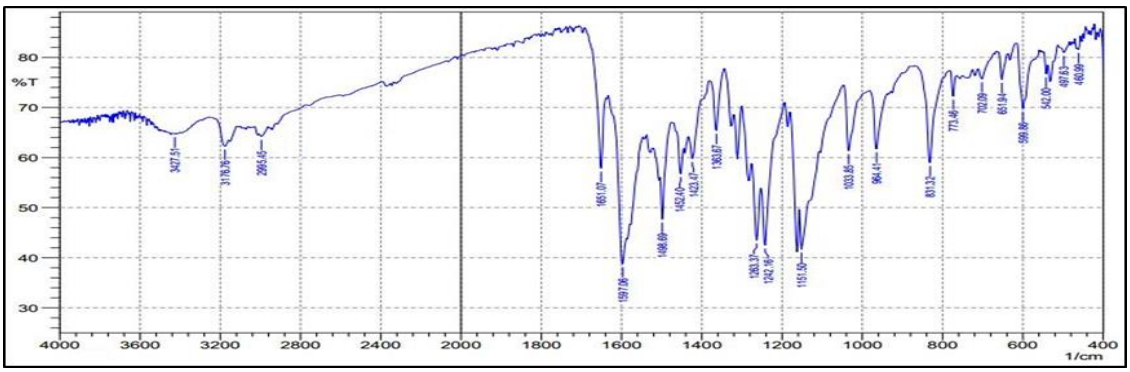

Figure 1. FT-IR spectrum of [NiL1L2Cl2]

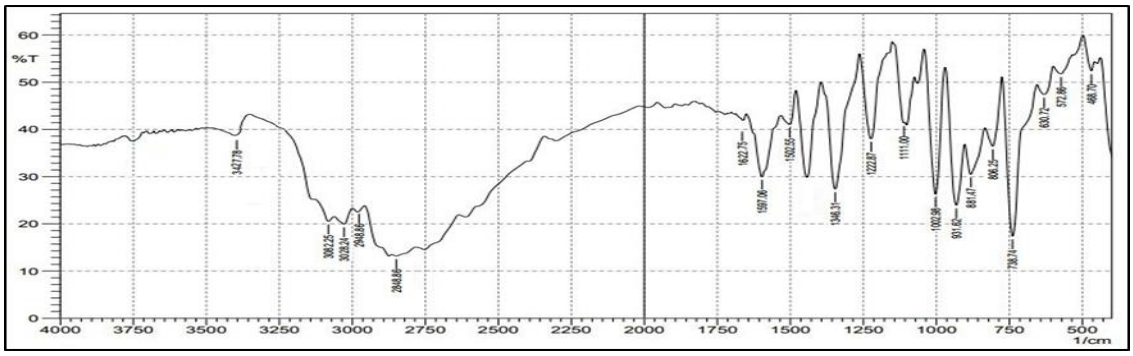

Figure (2). FT-IR spectrum of [CoL1L2Cl2]

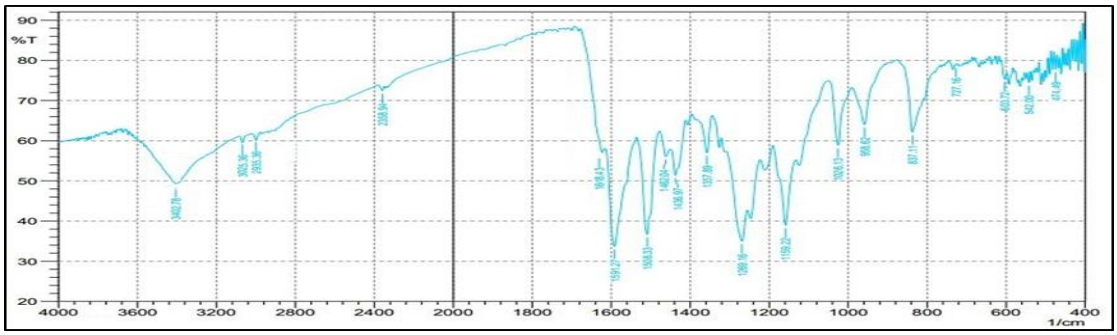

Figure 3. FT-IR spectrum of [ZnL1L2Cl2]

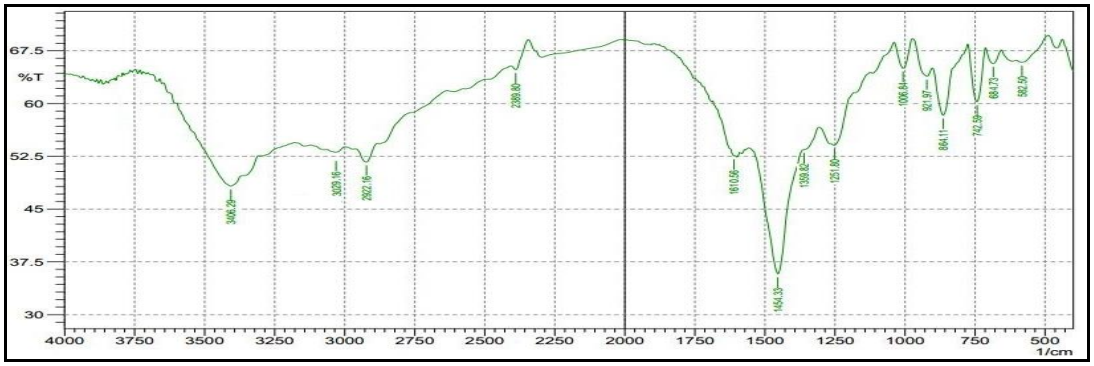

Figure 4. FT-IR spectrum of [CuL1L2Cl2]

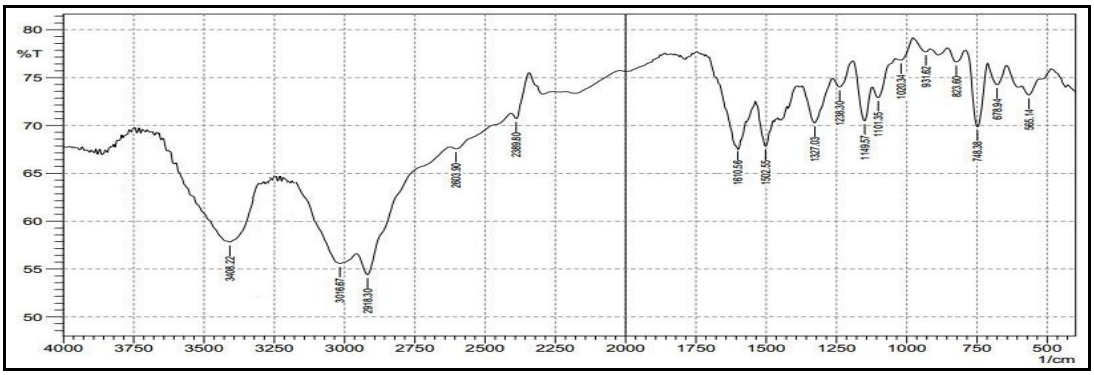

Figure(5). FT-IR spectrum of [MnL1L2Cl2]

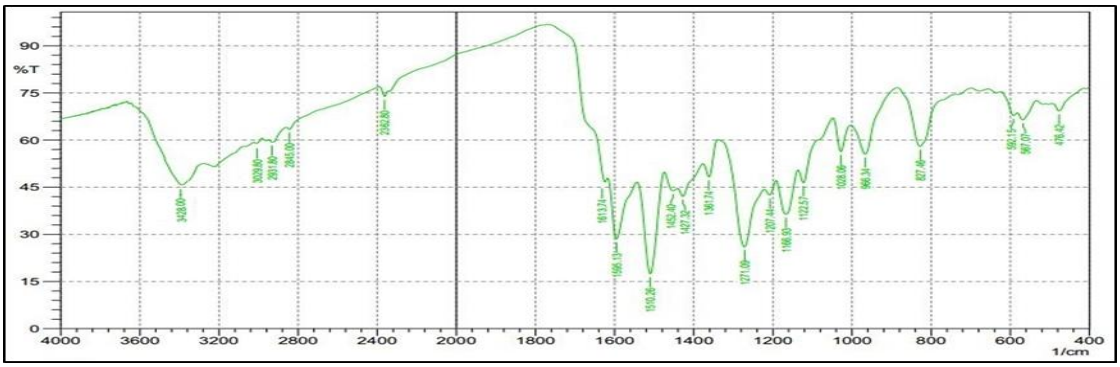

Figure 6. FT-IR spectrum of [CdL1L2Cl2]

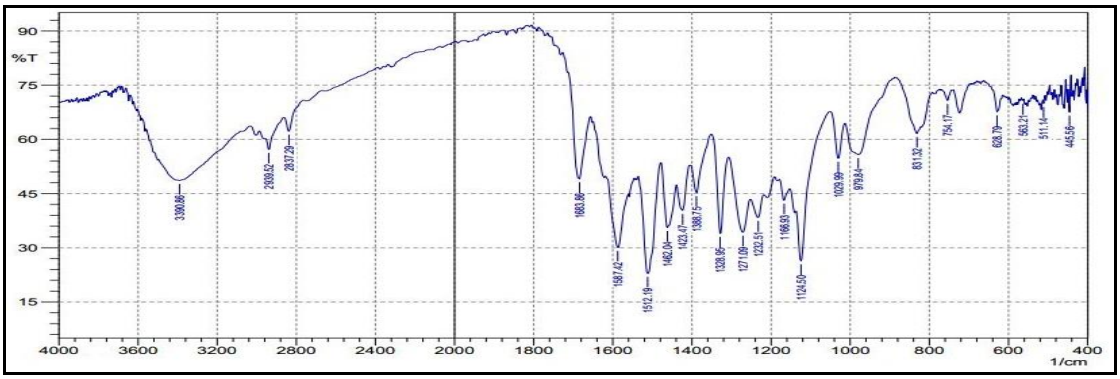

Figure 7. FT-IR spectrum of [FeL1L2Cl2]Cl

UV-Vis spectra, mass Spectrum, molar conductivity and magnetic susceptibility

The UV-Vis spectra of the prepared compounds were measured in DMSO solvent (1×10-3 M) at room temperature. The UV-Vis spectra of [NiL1L2Cl2] displayed six absorption bands (Fig. 6). The first band was at 542 nm (18450 cm-1) which is assigned to 3A2g→3T1g(F) electronic transition. The second band was at 505 nm (19801 cm-1) and attributed to 3A2g→3T1g(P) electronic transition another band was at 324 nm (31948 cm-1) and attributed to M→LCT electronic transition. The fourth band was at 313 nm (30864 cm-1) which is assigned to n→π* electronic transition, and another band was at 280 nm (35714 cm-1) and attributed to π→π* electronic transition. An absorption peak at (264 nm) (37878 cm-1) is due to the electron transition π→π*, which is attributed to the octahedral shape (Al-Hamdani et al.,2015). for the complex [NiL1L2Cl2.H2O], The mass spectrum of the [NiL1L2Cl2] a peak at m/z 415which represents the molecular weight of the compound (C16H17NCl2NiO4) (M+). The ultraviolet spectrum of the [CoL1L2Cl2] complex (Figure-7) in DMSO solvent showed absorption peaks at (683 nm) (14641) cm-1 (which belong to the electron transition 4T1g →4A2g), and also a broad

peak at (437 nm) (22883 cm-1) which belongs to the electron transition 4T1g →4T1g (P) as well as absorption peak at (329 nm) (30395 cm-1) which is due to the electron transition M→LCT, n→π* and an absorption peak at (297 nm) (33670 cm-1) that belongs to the electron transition π→π*, which is attributed to the octahedral shape [CoL1L2Cl2.H2O][19]. The ultraviolet spectrum of the [CuL1L2Cl2] complex showed absorption peaks at (419 nm) 23866) cm-1 (which is due to the electron transition 2Eg →2T2g) and at (297 nm) (33670 cm-1) which is obtained from the electron transition n→π* also an absorption peak at (258 nm) 38759 cm-1. This is due to the electronic transition π→π*, which is attributed to the octahedral shape (Kareem et al.,2021), as shown in Figure (3-25).

The ultraviolet spectrum of the [FeL1L2Cl2]Cl complex showed absorption peaks at (800 nm) (12500) cm-1 (which are results from the electronic transmission 6A1g→4T1g(G) and at (665 nm) (15037) cm-1) which are due to the electronic transmission 6A1g→4T2g(G) and an absorption peak at (426 nm) (23474) cm-1) which is due to the electron transition 4Eg(G),6A1g→4A1g and an absorption peak at (290 nm) (34482) cm-1) which is due to the transition results from this transition to octahedral shape (Rosu et al., 2021) also the mass spectrum of [FeL1L2Cl2]Cl compound, a peak at m/z 413, which represents the molecular weight of the compound,(C16H17NCl3FeO4) (M+). [ZnL1L2Cl2] complex showed absorption peaks at (379 nm) (26385) cm-1 (which is due to the M→LCT electron transition) and at (293 nm) (34129 cm-1) which is results from the n→π* electron transition, and an absorption peak at (279 nm) 35842 cm-1 that belongs to the electronic transition π→π*, which is attributed to this transition to the octahedral shape (Da Silva et al.,2021) , the mass spectrum of [ZnL1L2Cl2] compound showed a peak at m/z 421, which represents the molecular weight of the compound (C16H17NCl2ZnO4) (M+).

The [CdL1L2Cl2] complex has absorption peaks at (377 nm) (26525 cm-1) which are due to the electron transition (M→LCT) and at (308 nm) (32467 cm-1) which belong to the electron transition (n→π*), which is attributed to the octahedral shape(Obaid et al.,2020). ,the mass spectrum of [CdL1L2Cl2] compound, a peak at m/z 470.96, which represents the molecular weight of the compound, (C16H17NCl2CdO4) (M+), also showed the ultraviolet spectrum of the [MnL1L2Cl2] complex has absorption peaks at (632 nm) 15822 cm-1 (which belong to the electron transition 6A1g→4T1g (G) and at (609 nm) 16420 cm-1) which belongs to the electron transition 6A1g→4T2g(G) and an absorption peak at (591 nm) (16920) cm-1. Which belongs to

the electron transition 6A1g→4A1g, 4Eg(G) and an absorption peak at (423 nm) (23640 cm-1) that belongs to the electron transition M→LCT and at (305 nm) (32786 cm-1) that belongs to the electron transition n→π* And an absorption peak at (289 nm) (34602) cm-1, which is due to the electron transition π→π*, which is attributed to the octahedral shape (Obaid et al., 2020). The spectral charts UV-Vis spectra for all complexes prepared and Figure (9) showing the spectral charts mass spectra for all complexes prepared.

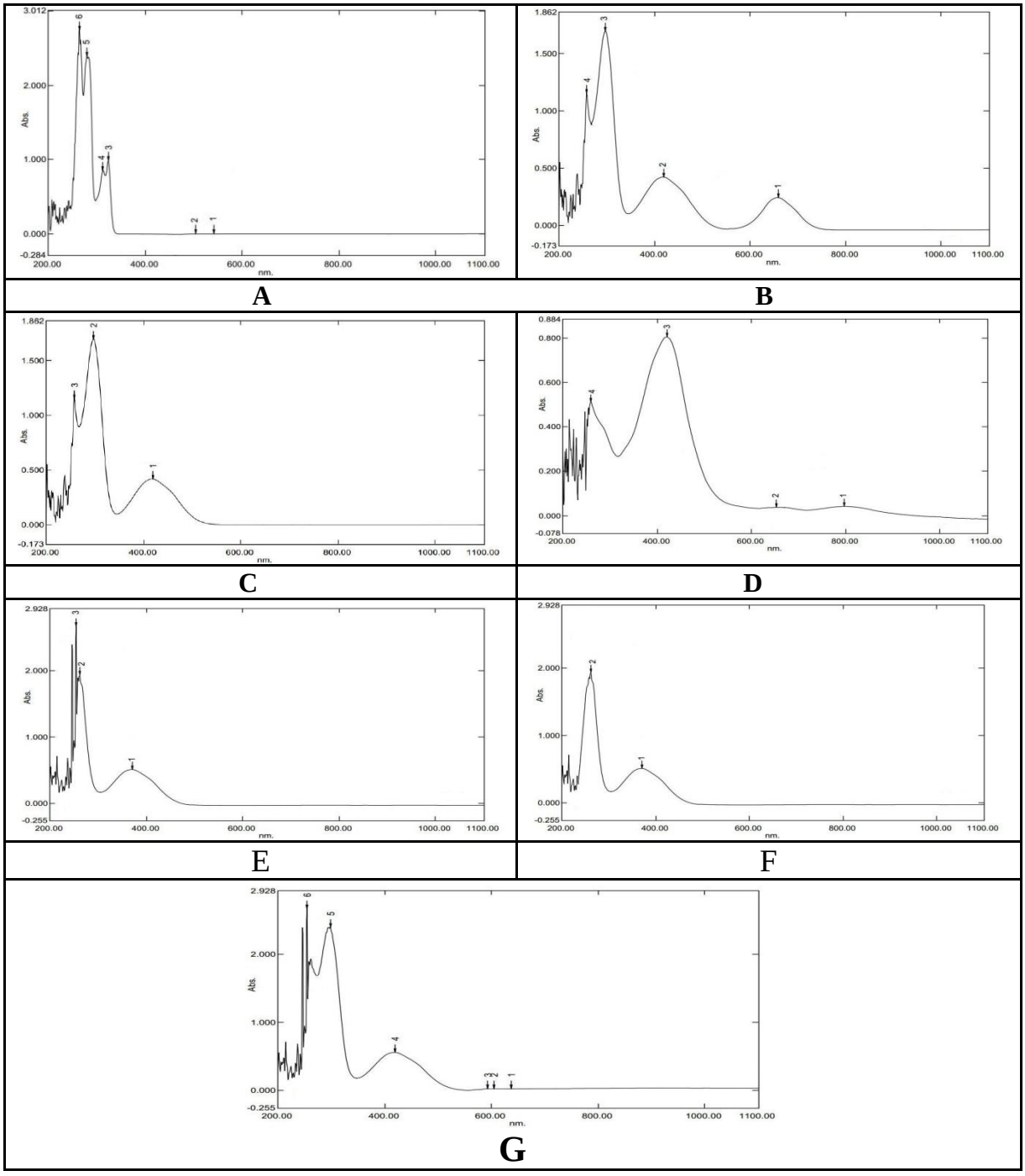

Figure 8. UV-vis spectrum of (A- [NiL1L2Cl2]), (B- [CoL1L2Cl2]), (C- [ZnL1L2Cl2]), (D- [CuL1L2Cl2]), (E- [MnL1L2Cl2]), (F- [CdL1L2Cl2]) and (G- [FeL1L2Cl2]Cl) in DMSO at 10-3M

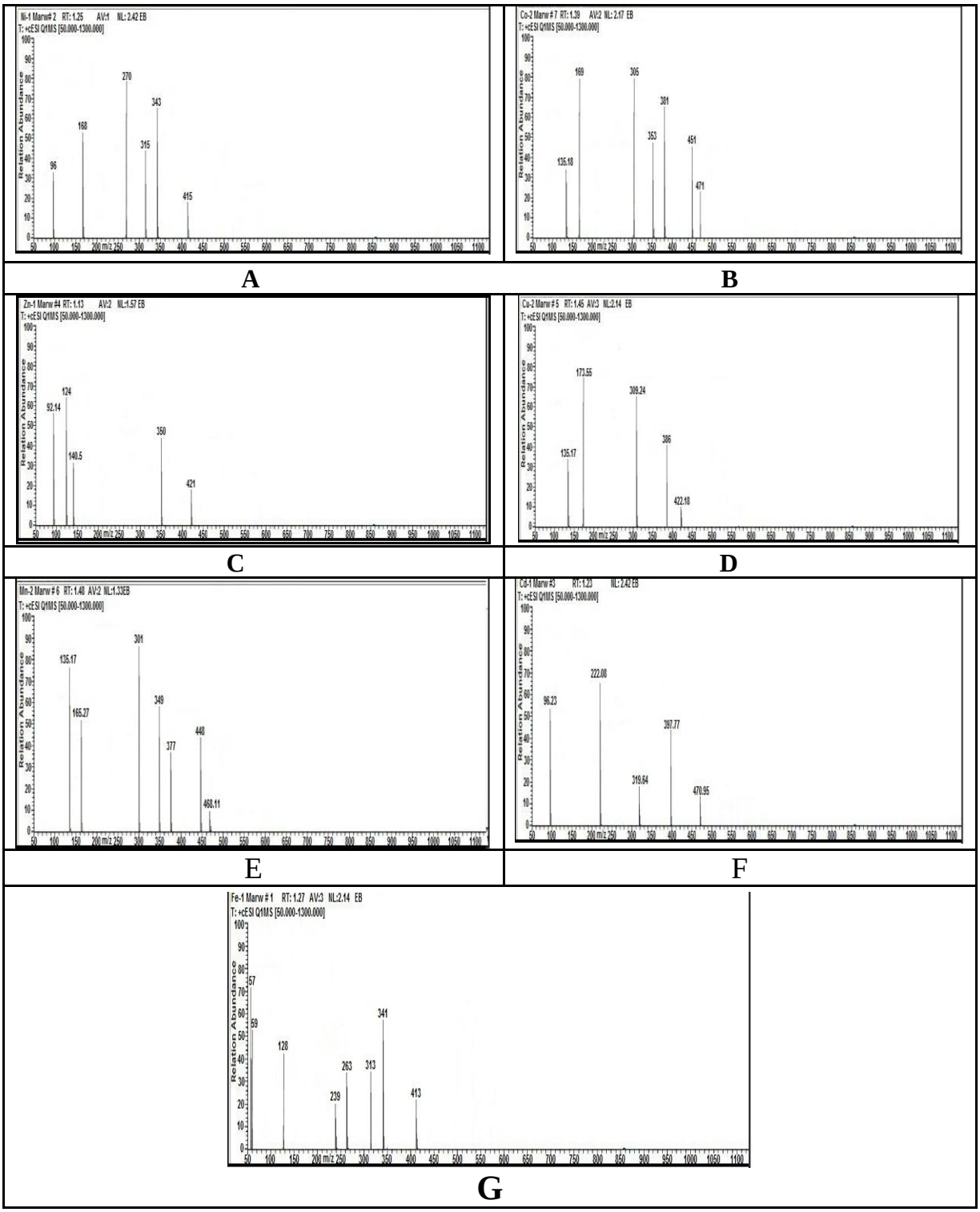

Figure 9. Mass spectrum of (A- [NiL1L2Cl2]), (B- [CoL1L2Cl2]), (C- [ZnL1L2Cl2]), (D- [CuL1L2Cl2]), (E- [MnL1L2Cl2]), (F- [CdL1L2Cl2]) and (G- [FeL1L2Cl2]Cl)

Molar conductivity and magnetic properties for complexes

The measured molar conductivity is (17, 13, 21, 20, 19, 11 and 48) Λm (S.cm2.mol-1) for [Ni(II), Co(II), Zn(II), Cu(II), Mn(II), Cd(II) and Fe(II)] complexes (Geary,2971). The magnetic measure was of the prepared [MnL1L2Cl2] complex shown in Table 1, the magnetic value 5.71 B.M., This agreement with octahedral geometry around Mn(II) ion. Measurements of the prepared [FeL1L2Cl2]Cl complex showed Table 1 the magnetic value 5.48 B.M., This agreement with octahedral geometry around Fe(II) ion. The magnetic value is 3.718 B.M. of [CoL1L2Cl2], this agreement with octahedral geometry around the Co(II) ion. Measurements of the prepared [NiL1L2Cl2] complex showed Table 1 the magnetic value 2.128 B.M., This agreement with octahedral geometry around Ni(II) ion. The magnetic value 1.66 B.M. of CuL1L2, this agreement with the octahedral geometry around the Cu(II) ion. The ([ZnL1L2Cl2] and [CdL1L2Cl2]) complexes have diamagnetic properties (Gatteschi et al.,2012).

Table 5. Molar conductivity measurements of metallic complexes

Comp.	Λm ($S.cm^2.Mol^{-1}$)
$[NiL_1L_2Cl_2]$ = 416.91	17
$[CoL_1L_2Cl_2]$ = 417.15	13
$[ZnL_1L_2Cl_2]$ = 423.61	21
$[CuL_1L_2Cl_2]$ = 421.76	20
$[MnL_1L_2Cl_2]$ = 413.15	19
$[CdL_1L_2Cl_2]$ = 470.96	11
$[FeL_1L_2Cl_2]Cl$ = 414.06	48

Table 6. The magnetic value of the metal complexes

No.	Comp.	effective magnetic (Prac.) moment μ_{eff} (B.M)	Effective magnetic moment (Theor.) μ_{eff}(B.M)	expected shape	Hybridization
1	$[MnL_1L_2Cl_2]$	5.71	5.916	Octahedral	sp^3d^2
2	$[FeL_1L_2Cl_2]Cl$	5.48	5.916	Octahedral	sp^3d^2
3	$[CoL_1L_2Cl_2]$	3.718	3.872	Octahedral	sp^3d^2
4	$[NiL_1L_2Cl_2]$	2.128	2.828	Octahedral	sp^3d^2
5	$[CuL_1L_2Cl_2]$	1.66	1.732	Octahedral	sp^3d^2
6	$[ZnL_1L_2Cl_2]$	Diamagnetic	0	Octahedral	sp^3d^2
7	$[CdL_1L_2Cl_2]$	Diamagnetic	0	Octahedral	sp^3d^2

Antimicrobial activity

The present research summarized the synthesis of Mixed ligand complexes. The complexes were screened against several bacterial species and fungi, figure (10) showed the zones of inhibition against bacteria and fungi and exhibited promising antimicrobial agents. Complexes ([FeL1L2Cl2]Cl, [MnL1L2Cl2], [ZnL1L2Cl2]) showed more activity against E.coli, Spuedomonas (gram-negative) and Staph. aureas, Bacillus (gram-positive) than other complexes according to the prepare conc. as shown in table(7). Complexe [CoL1L2Cl2] (0.0048 mg/ml) had higher antifungal activity than the rest of the complexes that were inactive against these types of fungi (Fuzarium, Aspergillus.) as shown in table 8 and the complex [CdL1L2Cl2] (0.0095 mg/ml) gave only effective action against Aspergillus**.**

Table 7. Inhibition zone for the M(L1)(L2) complexes against several bacterial species

Sample	mg/ml	Gram positive		Gram negative	
		Staph. aureas **Inhibition zone cm**	***Bacillus*** **Inhibition zone cm**	***Spuedomonas*** **Inhibition zone cm**	***E. Coli*** **Inhibition zone cm**
$[CoL_1L_2Cl_2]$	0.0048	-ve	1.2	1	1.8
$[NiL_1L_2Cl_2]$	0.0018	-ve	-ve	1.2	1.5
$[CuL_1L_2Cl_2]$	0.0063	1.5	-ve	-ve	2
$[CdL_1L_2Cl_2]$	0.0095	-ve	1.7	1.5	2.1
$[FeL_1L_2Cl_2]Cl$	0.0013	1.5	2	1.2	2.5
$[MnL_1L_2Cl_2]$	0.0063	1.3	1.5	1.3	2
$[ZnL_1L_2Cl_2]$	0.008	1.6	1.7	1	2.5

Table 8. Inhibition zone for the M(L1)(L2) complexes against several fungi (Fuzarium, Aspergillus.) species

Sample	mg/ml	***Aspergillus niger*** **growth cm**	***Fuzarium*** **growth cm**
$[CoL_1L_2Cl_2]$	0.0048	2.8	2.5
$[NiL_1L_2Cl_2]$	0.0018	-ve	-ve
$[CuL_1L_2Cl_2]$	0.0063	-ve	-ve
$[CdL_1L_2Cl_2]$	0.0095	3.3	-ve
$[FeL_1L_2Cl_2]Cl$	0.0013	-ve	-ve
$[MnL_1L_2Cl_2]$	0.0063	-ve	-ve
$[ZnL_1L_2Cl_2]$	0.008	-ve	-ve

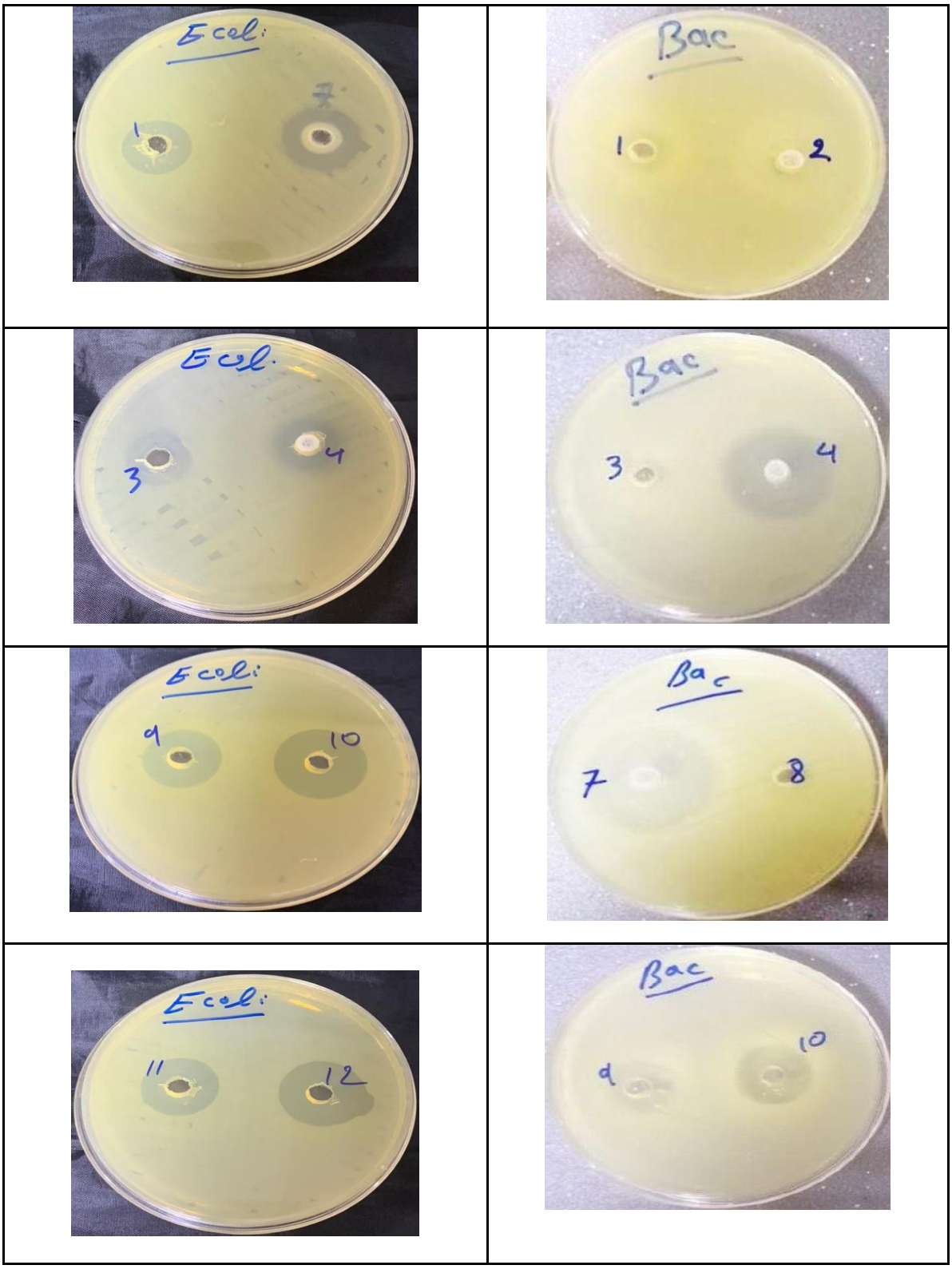

Figure 10. Antibacterial activity image, ML1L2 complexes against Esherichia Coli, Bacillus

Conclusions

The metal salts (M=Co(II), Ni(II), Cu(II), Mn(II), Zn(II), Cd(II) and Fe(II) complexes of the mixed ligands were synthesized and characterized using C.H.N.O.S elemental analysis, FT-IR, UV-visible, mass spectrum, molar conductivity, magnetic susceptibility and Conductivity measurements. The results of infrared spectroscopy clearly elucidated that the Dimedon (L1) as a primary ligand and Isatin (L2) ligands coordinate with metal ions as monodentate via oxygen atoms by the two oxygen atoms of Dimedon (L1) and Isatin (L2) molecule. All the complexes have octahedral geometry, the complexes (Co(II), Ni(II), Cu(II), Mn(II) and Fe(II) have a paramagnetic property while the Cd(II) and Zn(II) complexes have a diamagnetic property. The antimicrobial activity of the metal complexes indicated that all the prepared metal complexes have no effects on Fuzarium fungi, however, they largely affected the growth of Escherichia Coli and Pseudomonas bacteria.

Acknowledgement

The authors would like to thank, Anbar University and, the Ministry of Higher Education and Scientific Research for supporting the present work.

References

Al-Hamdani, A. A. S., BALKHI, A., Falah, A., & Shaker, S. A. (2015). New azo-Schiff Base derived with Ni (II), Co (II), Cu (II), Pd (II) and Pt (II) complexes: preparation, spectroscopic investigation, structural studies and biological activity. Journal of the Chilean Chemical Society, 60(1), 2774-2785.

Al-Hazmi, G. A., Abou-Melha, K. S., Althagafi, I., El-Metwaly, N., Shaaban, F., Abdul Galil, M. S., & El-Bindary, A. A. (2020). Synthesis and structural characterization of oxovanadium (IV) complexes of dimedone derivatives. Applied Organometallic Chemistry, 34(8), e5672.

Cozzi, P. G. (2004). Metal–Salen Schiff base complexes in catalysis: practical aspects. Chemical Society Reviews, 33(7), 410-421.

Da Silva, C. M., da Silva, D. L., Modolo, L. V., Alves, R. B., de Resende, M. A., Martins, C. V., & de Fátima, Â. (2011). Schiff bases: A short review of their antimicrobial activities. Journal of Advanced research, 2(1), 1-8.

Fatima, F., Bhat, S. H., Ullah, M. F., Abu-Duhier, F., & Husain, E. (2018). In-Vitro Antimicrobial Activity of Herbal Extracts From Tabuk Region (Kingdom of Saudi Arabia) Against Nosomial Pathogens: A Preliminary Study. Global Journal of Health Science, 10(3), 83.

Gatteschi, D., Kahn, O., Miller, J. S., & Palacio, F. (Eds.). (2012). Magnetic molecular materials (Vol. 198). Springer Science & Business Media.

Geary, W. J. (1971). The use of conductivity measurements in organic solvents for the characterisation of coordination compounds. Coordination Chemistry Reviews, 7(1), 81-122.

Hegade, S., Gaikwad, G., Jadhav, Y., Pore, A., & Mulik, A. (2022). Catalytic one-pot three-component synthesis of 3, 3′-disubstituted oxindoles and spirooxindole pyrans by mixed ligand transition metal complexes. Monatshefte für Chemie-Chemical Monthly, 153, 95-103.

Ibrahim, A. A. J. (2011). Synthesis and characterization of mixed ligand complexes of some metal chlorides with 8-hydroxyquinoline and amino acid (L-lysine). Diyala Journal for Pure Sciences, 7.

Jirjees, V. Y., Al-Hamdani, A. A. S., Wannas, N. M., A. R, F., Dib, A., & Al Zoubi, W. (2021). Spectroscopic characterization for new model from Schiff base and its complexes. Journal of Physical Organic Chemistry, 34(4), e4169.

JMOZINGO JR, J. R. (1968). A study of bicyclic furans and thiophenes. The University of Mississippi.

Kareem, M. J., Al-Hamdani, A. A. S., Jirjees, V. Y., Khan, M. E., Allaf, A. W., & Al Zoubi, W. (2021). Preparation, spectroscopic study of Schiff base derived from dopamine and metal Ni (II), Pd (II), and Pt (IV) complexes, and activity determination as antioxidants. Journal of Physical Organic Chemistry, 34(3), e4156.

Matuschek, E., Brown, D. F., & Kahlmeter, G. (2014). Development of the EUCAST disk diffusion antimicrobial susceptibility testing method and its implementation in routine microbiology laboratories. Clinical microbiology and infection, 20(4), O255-O266.

Numan, A. T. (2015). Synthesis and Characterization of some biologically active transition metal complexes for a ligand derived from dimedone with mixed ligands. *Journal of the college of basic education*, *21*(88), 25-36.

Numan, A. T., Ali, K. F., & Al-salihi, E. I. (2017). Synthesis and Characterization of Schiff Base Folic Acid Based Ligand and Its Complexes. Ibn AL-Haitham Journal For Pure and Applied Science, 28(2), 69-85.

Obaid, S. M., Jarad, A. J., & Al-Hamdani, A. A. S. (2020, November). Synthesis, characterization and biological activity of mixed ligand metal salts complexes with various ligands. In Journal of Physics: Conference Series (Vol. 1660, No. 1, p. 012028). IOP Publishing.

Pandeya, S. N., Smitha, S., Jyoti, M., & Sridhar, S. K. (2005). Biological activities of isatin and its derivatives. *Acta Pharm*, *55*(1), 27-46.

Patange, V. N., Pardeshi, R. K., & Arbad, B. R. (2008). Transition metal complexes with oxygen donor ligands: a synthesis, spectral, thermal and antimicrobial study. Journal of the Serbian Chemical Society, 73(11), 1073-1082.

Rao, T. N., Krishnarao, N., Ahmed, F., Alomar, S. Y., Albalawi, F., Mani, P., ... & Kumar, S. (2021). One-Pot Synthesis of 7, 7-Dimethyl-4-Phenyl-2-Thioxo-2, 3, 4, 6, 7, 8-Hexahydro-1H-Quinazoline-5-OnesUsing Zinc Ferrite Nanocatalyst and Its Bio Evaluation. Catalysts, 11(4), 431.

Rosu, T., Pahontu, E., Maxim, C., Georgescu, R., Stanica, N., & Gulea, A. (2011). Some new Cu (II) complexes containing an ON donor Schiff base: Synthesis, characterization and antibacterial activity. Polyhedron, 30(1), 154-162.

Tadayon, M., & Garkani-Nejad, Z. (2019). Quantitative structure–activity relationship study using genetic algorithm–enhanced replacement method combined with molecular docking studies of isatin derivativesas inhibitors of human transglutaminase 2. Journal of the Chinese Chemical Society, 66(3), 265-277.

Taghreed, H., Lekaa, K., & Al-Noor, T. H. (2016). synthetic, spectroscopic and antibacterial studies of Co (II), Ni (II), Cu (II), Zn (II), Cd (II) and Hg (II), mixed ligand complexes of trimethoprime antibiotic and anthranilic acid. TOFIQ Journal of Medical Sciences (TJMS), 64.

Teixeira, A. M. R., Santos, H. S., Bandeira, P. N., Julião, M. S. S., Freire, P. T. C., Lima, V. N., ... & Sena Jr, D. M. (2019). Structural, spectroscopic and microbiological characterization of the chalcone 2E-1-(2′-hydroxy-3′, 4′, 6′-trimethoxyphenyl)-3-(phenyl)-prop-2-en-1-one derived from the natural product 2-hydroxy-3, 4, 6-trimethoxyacetophenone. Journal of Molecular Structure, 1179, 739-748.

Vandana, K., Marathakam, A., Thushara, B. S., & Rajitha, K. (2017). A Review on Isatin Derivatives With Diverse Biological Activites. World Journal of Pharmaceutical Research, 6(16), 318-332.

Yilmaz, V. T., & Topcu, Y. (1997). Preparation, characterization and thermal reactivity of N, N-dimethylformamide complexes of some transition metal chlorides. Thermochimica acta, 307(2), 143-147.